Available online at www.sciencedirect.com
ScienceDirect
Journal of Power Sources 174 (2007) 1086–1090
JOURNAL OF POWER SOURCES
www.elsevier.com/locate/jpowsour

Short communication

XPS study of electrode/electrolyte interfaces of η-Cu_6Sn_5 electrodes in Li-ion batteries

S. Naille [a], R. Dedryvère [b,*], H. Martinez [b], S. Leroy [b], P.-E. Lippens [a], J.-C. Jumas [a], D. Gonbeau [b]

[a] *LAMMI, Université Montpellier II, Place Eugène Bataillon, CC015, 34095 Montpellier Cedex 5, France*
[b] *LCTPCM, Université de Pau, Hélioparc Pau Pyrénées, 2 av. Pierre Angot, 64053 Pau Cedex 9, France*

Available online 23 June 2007

Abstract

Research into new negative electrode materials as an alternative to carbonaceous materials brings new questions about electrode/electrolyte interface mechanisms. For graphite, these mechanisms have great importance on the ageing phenomena. What about intermetallic alloys, such as Cu–Sn systems? The nature of the electrode and its potential of lithium ions uptake (different from graphite) may have a great influence on the passivation film formed at the surface of the electrode. In this paper, we report on the XPS study of the electrode/electrolyte interface of a Cu_6Sn_5-based electrode. The main difference with graphite is not the nature and composition of the passivation layer, but its poor dependence on the electrochemical reaction during cycling.

Keywords: XPS; Cu_6Sn_5; Intermetallic alloys; Interfaces

1. Introduction

Most commercial rechargeable lithium batteries currently use carbonaceous materials as negative electrode. Research on new negative electrode materials has increased over the past few years, in order to find a substitute for carbonaceous electrodes. These new materials must show improved capacities and intercalation potentials higher than that of the Li^+/Li redox couple, in order to minimize the risks of metallic lithium dendrite growth on the electrode surface that causes security problems [1].

The result of these research projects has led to the development of new alternative materials such as lithium–metal alloys, especially lithium–tin alloys, which have great specific capacities and higher lithium insertion voltages than Li^+/Li, which reduces safety concerns [2,3]. The Li–Sn phase diagram shows the existence of seven intermetallic phases: Li_2Sn_5, LiSn, Li_7Sn_3, Li_5Sn_2, $Li_{13}Sn_5$, Li_7Sn_2 and $Li_{22}Sn_5$ [4]. However, cycling performance of these alloys rapidly deteriorates due to a large Li-driven volume change (up to 300% when 4.4Li per Sn atom are inserted). This volume expansion causes mechanical stress of the electrode material and thus leads to a loss of electrical contacts between particles [5].

Intermetallic compounds, that undergo a metal displacement reaction upon lithium insertion, stand as possible alternative negative electrode materials, such as, for example, Cu_6Sn_5 [6]. In these compounds, the active element (Sn, in our case) reacts with lithium to form a lithium alloy, while the inactive material (Cu, in our case) plays the role of a matrix buffering the volume expansion. Based on this principle, Cu_6Sn_5 could be a promising anode material. This compound undergoes an ordering change between 186 and 189 °C and the decomposition of the high temperature phase happens at 415 °C [7,8]. The high temperature phase η-Cu_6Sn_5 crystallizes in the hexagonal-type system (space group $P6_3/mmc$), with the conventional NiAs structure.

Current research tasks tend to optimize the synthesis conditions of this material (direct high temperature synthesis, high energy ballmilling procedure, chemical reduction method, etc.) [6,9,10] in order to control particles size that enhances mechanical performance of electrodes. Special attention has also been paid to the understanding of the electrochemical mechanisms during alloying reactions with lithium [10–12]. Choi et al. have recently proposed a three-step reaction mechanism [13]:

$$Cu_6Sn_5 + xLi \rightarrow Li_xCu_6Sn_5 \quad (x < 3Li) \tag{1}$$

* Corresponding author.
E-mail address: remi.dedryvere@univ-pau.fr (R. Dedryvère).

0378-7753/$ – see front matter © 2007 Elsevier B.V. All rights reserved.
doi:10.1016/j.jpowsour.2007.06.043

$$Li_xCu_6Sn_5 + (10 - x)Li \rightarrow 5Li_2CuSn + Cu \quad (2)$$

$$2Li_2CuSn + 3Li \rightarrow Li_7Sn_2 + 2Cu \quad (3)$$

Reaction (1) forms a Li solid solution in Cu_6Sn_5 up to 0.4 V versus Li^+/Li. The two-phase reaction (2) occurs at 0.4 V versus Li^+/Li and finally a displacement reaction (3) takes place up to 0.01 V versus Li^+/Li. The Li_2CuSn phase can be highlighted by X-ray diffraction, and the Li_7Sn_2 phase has been characterized by electron diffraction from transmission electron microscopy. On the other hand, an uncertainty remains about the reversibility of these processes.

Concerning electrode/electrolyte interface mechanisms, very few studies have been carried out to identify the species that are formed at the surface of Cu_6Sn_5-based electrodes, and to display the influence of the potential change on the surface film formation with respect to graphite. However, several works have been aimed at characterizing the passivation films at the surface of SnO-based electrodes, in which it is well known that lithium insertion leads to Li_xSn alloys that should be similar to those formed with Cu_6Sn_5 [14,15]. Some similarities are therefore expected. These studies have shown the presence of carbonated species Li_2CO_3 and/or $ROCO_2Li$ at the surface of SnO particles during reaction with lithium [16,17].

Other works have shown the formation of a passivation film at the surface of other alloys such as Sn–Sb by means of infrared spectroscopy or scanning electron microscopy [18]. A formation model of the solid electrolyte interphase (SEI) has even been proposed by comparison with graphite [19]. The formation of a SEI is described as a possibility to partially explain the capacity fading observed upon cycling with this kind of electrodes, taking as reference the mechanisms commonly admitted for graphite.

However, very few studies have tried to fully characterize the species formed at the surface of these alloys and to understand the formation mechanisms of the passivation layer, as well as the influence of the potential on the step-by-step mechanisms. In this paper, the surface of Cu_6Sn_5-based electrodes used in Li/Cu_6Sn_5 cells has been investigated by X-ray photoelectron spectroscopy (XPS).

2. Experimental

The pristine material η-Cu_6Sn_5 was synthesized directly from pure elements in silica tube sealed under vacuum. After annealing for 1 week at 400 °C, the tube sample was quenched at ice temperature. The pristine material was synthesized with a composition of 43.5 at.% Sn.

The as-prepared η-Cu_6Sn_5 was characterized by X-ray powder diffraction, for phase identification and purity, with a Phillips θ–2θ diffractometer using Cu Kα radiation ($\lambda = 1.5418$ Å) and a nickel filter.

Electrochemical lithium insertion/extraction tests were performed in Swagelok^{TM}-type cells assembled in an argon-filled glove box. Positive electrodes were prepared by mixing 90 wt.% Cu_6Sn_5 powder, 5 wt.% carbon black and 5 wt.% PTFE binder and pressed in 7 mm diameter pastilles. The electrolyte was 1 M $LiPF_6$ in EC/PC/DMC (1:1:3, v/v/v). The experiments were performed galvanostatically at a *C*/20 rate (1Li/20 h), using a Mac Pile II system, within a voltage window of 0.01–1.5 V.

For surface studies, the electrodes were carefully separated from the rest of the battery components, washed with DMC to remove the electrolyte, and dried prior to being packed into a hermetical sealed glass tube for transportation. All the operation was done in a glove box under argon atmosphere. To prevent the samples from moisture/air exposure on the analysis site, the XPS spectrometer was directly connected through a transfer chamber to a nitrogen dry-box so that the electrodes could be easily removed from the tube within the dry-box, and placed on the sample holder without any contamination.

XPS analyses were carried out with a Kratos Axis Ultra spectrometer using a focused monochromatized Al Kα radiation ($h\nu = 1486.6$ eV). The analyzed area of the samples was 300 μm × 700 μm, and the pressure in the analysis chamber was ca. 5×10^{-7} Pa. Short-time spectra were recorded at the beginning and at the end of each experiment to check the non-degradation of the samples in the X-ray beam. The binding energy scale was calibrated from the carbon contamination using the C 1s peak at 285.0 eV. Core peaks were analyzed using a non-linear Shirley-type background, and peak positions and areas were obtained by a weighed least-square fitting of model curves (70% Gaussian, 30% Lorentzian) to the experimental data.

3. Results and discussion

To clearly make the difference between chemical reactivity of the electrode toward the electrolyte and electrochemical reactivity upon discharge or charge, the first experiment was to soak the electrode 24 h in the electrolyte. Fig. 1 shows XPS C 1s, F 1s, Sn $3d_{5/2}$ and Cu 2p core peaks of: (a) the pristine electrode and (b) after contact with the electrolyte.

Cu 2p core peak of the pristine electrode is characteristic of metallic copper. Sn $3d_{5/2}$ core peak shows two components: one at 484.9 eV assigned to Sn^0 and another one at 486.8 eV assigned to Sn^{IV}. The relative intensities of Cu^0 and Sn^0 signals are in good agreement with the Cu_6Sn_5 stoichiometry. Therefore, the Sn^{IV} component can be attributed to SnO_2: this means that 83% of tin is present in the form of SnO_2 at the surface of the electrode, due to a segregation effect resulting from the affinity of tin toward oxygen. It is worth noting that a so important part of oxide at the surface of the electrode will certainly have a consequence on its surface reactivity toward the electrolyte. Other core peaks (C 1s and F 1s) of the pristine electrode are characteristic of the additives, namely carbon black and PTFE.

XPS core peaks of the electrode after soaking are quite different. Cu 2p core peak is no more detectable. The Sn^0 signal also vanishes, showing a complete oxidation of the electrode surface. Moreover, the overall Sn $3d_{5/2}$ signal is divided by 40, which means that the electrode is covered by a surface film (let us recall that the XPS depth analysis is about 5 nm). This observation is confirmed by the C 1s core peak, since the signals of the electrode additives are no more detectable. Instead, three peaks can be observed: a first one at 285 eV assigned to hydrocarbon species, including hydrocarbon contamination. A second one at 290.1 eV assigned to carbonated species (Li_2CO_3 and/or

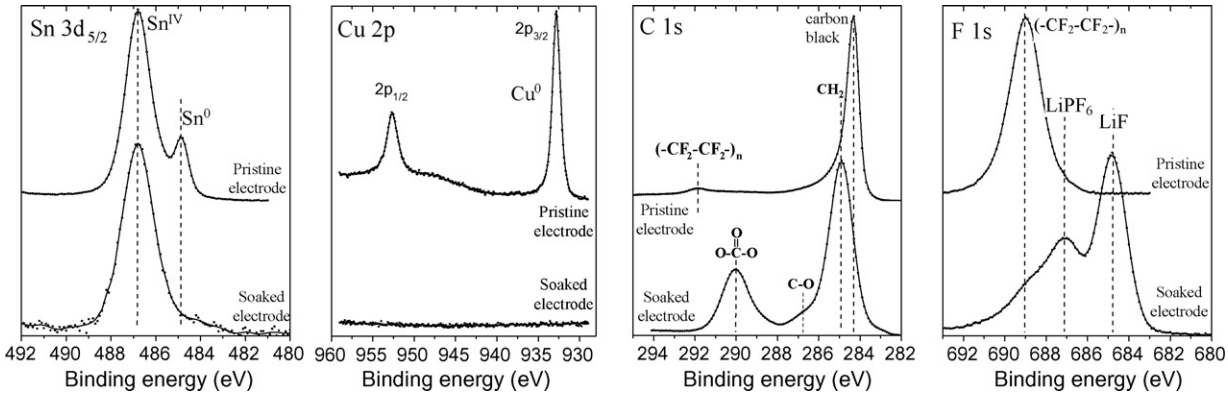

Fig. 1. XPS core peaks of the Cu_6Sn_5 electrode before and after soaking in the electrolyte.

$ROCO_2Li$), and a third one at 286–287 eV assigned to carbon atoms bound to only one oxygen. The low intensity of this latter shows that Li_2CO_3 is majority at the surface of the electrode, and that the amount of $ROCO_2Li$ is much lower.

F 1s core peak after soaking shows, beside a small shoulder peak at 689 eV assigned to PTFE binder, one component at 687 eV due to $LiPF_6$ and another one at 685 eV attributed to LiF. In summary, this proves that as soon as the first contact of the electrode several hours with the electrolyte, it is covered by a film containing Li_2CO_3 and LiF.

Fig. 2 shows the first discharge/charge cycle of the cell. Four electrochemical steps were studied: (a) at the beginning of the 0.4 V discharge plateau, (b) at the end of the 0.4 V discharge plateau, (c) at the end of discharge (0.01 V) and (d) after charge at 1.5 V. The results of XPS analysis of the electrode at these four steps are shown in Fig. 3.

C 1s core peak shows a similar profile for all samples. Indeed, two main peaks at 285 and 290 eV can be observed, respectively, assigned to hydrocarbon contamination and carbonates. As the component at 286–287 eV is very low, the amount of $ROCO_2Li$ still remains weak and the main carbonated species is Li_2CO_3. The quantitative analysis from XPS spectra shows

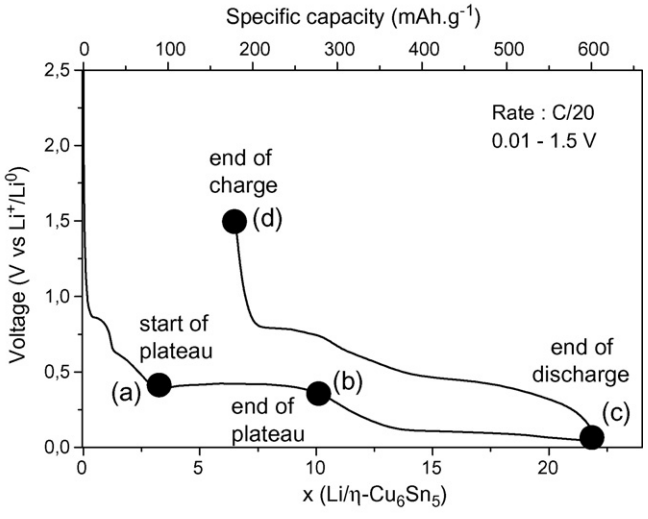

Fig. 2. First cycle of discharge/charge of a Li/η-Cu_6Sn_5 cell.

that the amount of Li_2CO_3 is rather stable over the first cycle (50–60%). This behaviour is completely different from that of a carbonaceous electrode, for which the potential of the cell has a great influence on the formation of Li_2CO_3 [20]. One can notice the appearance at the end of charge of a peak at 283.5 eV assigned to carbon black. This could be explained by a partial dissolution of the passivation layer at the surface of carbon black upon charge. This phenomenon is easy to understand if we consider that it is commonly observed at the surface of carbonaceous electrodes in usual $LiCoO_2$/graphite cells upon discharge. The peak at 292 eV due to PTFE is also hardly detectable.

F 1s core peak shows for all samples three peaks, respectively, assigned to PTFE, $LiPF_6$ and LiF. The quantitative analysis shows that the amount of LiF varies between 5 and 10% upon the first cycle, which is once again quite different from the behaviour of a carbonaceous electrode, since a great amount of LiF (>30%) is detected at the end of the Li insertion process [20].

P 2p spectra of the same samples show two components: one at 137 eV assigned to $LiPF_6$ and a second at 134 eV assigned to phosphates resulting from the salt decomposition. The relative intensity of the latter increases from (a) to (d), showing a progressive degradation of the salt upon the first cycle.

The analysis of valence spectra is very useful since it provides an image of all species present at the surface of the electrode together. When the surface film consists of a mixture of a few main compounds, the valence spectrum is rather simple to interpret. Thus, we can notice in Fig. 3 that all the characteristic peaks of Li_2CO_3 and LiF are observed in these spectra [21], which confirms the analysis of core peaks and proves that Li_2CO_3 and LiF are the main constituents of the interface. A very small peak at 17 eV can be assigned to a small amount of $ROCO_2Li$ species [21]. Other compounds are also present but in minority since they are not detected in the valence spectrum. Moreover, the composition of the interface does not significantly change upon the first cycle. The greatest valence peak of SnO_2 can also be observed at the beginning and at the end of the 0.4 V plateau, but quickly disappears upon discharge. This shows that the thickness of the film slightly increases during discharge, and does not decrease during the following charge.

Sn $3d_{5/2}$ core peak also brings some information. First, it remains detectable over all the first cycle, showing that the passivation film is never thick enough (>10 nm) to completely

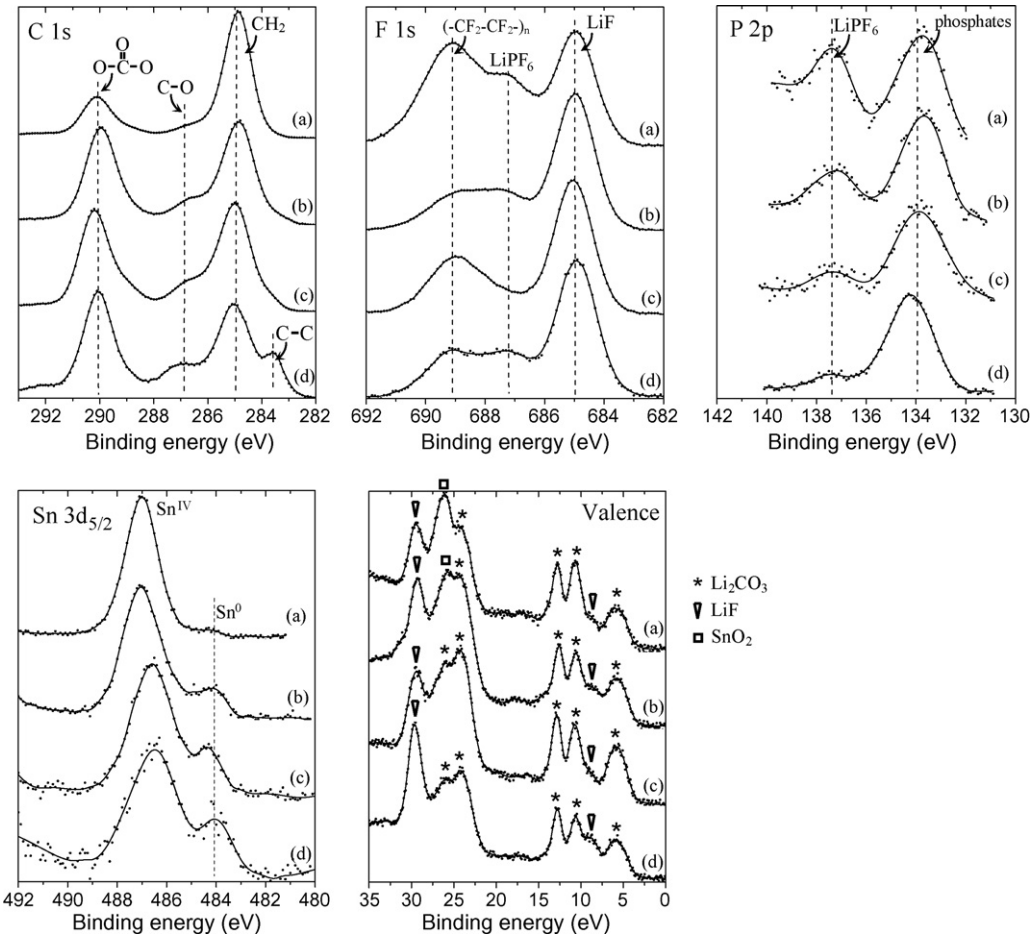

Fig. 3. XPS core peaks of the Cu_6Sn_5 electrode: (a) at the beginning of the 0.4 V plateau, (b) at the end of the 0.4 V plateau, (c) at the end of discharge and (d) at the end of charge.

hide the active material. However, the measured amount of tin (≈0.2–0.05%) is very low and decreases. Second, the Sn^0 component is observed at a lower binding energy (484.3 eV) than the pristine Cu_6Sn_5 (484.9 eV), which shows the alloying process to form Li_xSn. Finally, the relative intensity of Sn^0 with respect to Sn^{IV} increases upon discharge, showing the reaction of surface SnO_2 with lithium to form Li_xSn. After charge, we can notice that the binding energy value of the Sn^0 component is in good agreement with Li_xSn and not with Cu_6Sn_5 or metallic Sn. This result allows us to conclude that the alloying process is not totally reversible, and that the starting Cu_6Sn_5 phase cannot be recovered at the end of the first cycle. This lack of reversibility may concern only the very surface analyzed by XPS and not the bulk of alloy particles. Several mechanisms have already been proposed [19] to explain the residual presence of Li_xSn alloys at the end of charge: it could be due to a loss of electrical contact of some parts of the electrode as a result of volume changes during lithium insertion and extraction, leading to mechanical strain and cracking.

4. Conclusion

As a conclusion for this study, we have observed that the passivation layer at the surface of the Cu_6Sn_5 electrode forms as soon as the first contact with the electrolyte, contrary to a graphite electrode. The main difference with the graphite behaviour is not the nature and composition of the passivation layer (the same main species are detected: Li_2CO_3 and LiF), but that they are poorly dependent on the electrochemical reaction during cycling.

The formation of a passivation layer at the surface of this electrode can be explained by the greater reactivity of Cu_6Sn_5 toward the electrolyte with respect to graphite (the great amount of oxide at the surface may play an important role in this reactivity). However, the reason why the electrochemical reaction has a low influence on the passivation layer composition is still not clear. Further investigations are necessary to better understand electrode/electrolyte interface phenomena with this kind of systems, and it is absolutely not clear that the capacity fading observed upon the first cycle is due, as in the case of graphite, to the formation of a passivation layer at the surface of the electrode.

References

[1] J.M. Tarascon, M. Armand, Nature 414 (2001) 359–367.
[2] K.D. Kepler, J.T. Vaughey, M.M. Thackeray, J. Power Sources 81–82 (1999) 383–387.
[3] M. Winter, J.O. Besenhard, Electrochim. Acta 45 (1999) 31–50.

[4] F. Robert, P.E. Lippens, J. Olivier-Fourcade, J.C. Jumas, F. Gillot, M. Morcrette, J.M. Tarascon, J. Solid State Chem. 180 (2007) 413–422.
[5] M. Winter, J.O. Besenhard, M.E. Spahr, P. Novák, Adv. Mater. 10 (1998) 725–763.
[6] L. Fransson, E. Nordström, K. Edström, L. Häggström, J.T. Vaughey, M.M. Thackeray, J. Electrochem. Soc. 149 (2002) A736–A742.
[7] A.K. Larsson, L. Stenberg, S. Lidin, Acta Cryst. B 50 (1994) 636–643.
[8] A. Ganguluee, G.C. Das, M.B. Bever, Metall. Trans. 4 (1973) 2063–2066.
[9] G.X. Wang, L. Sun, D.H. Bradhurst, S.X. Dou, H.K. Liu, J. Alloys Compd. 299 (2000) L12–L15.
[10] J. Wolfenstine, S. Campos, D. Foster, J. Read, W.K. Behl, J. Power Sources 109 (2002) 230–233.
[11] M.M. Thackeray, J.T. Vaughey, C.S. Johnson, A.J. Kropf, R. Benedek, L.M.L. Fransson, K. Edström, J. Power Sources 113 (2003) 124–130.
[12] S. Sharma, L. Fransson, E. Sjöstedt, L. Nordström, B. Johansson, K. Edström, J. Electrochem. Soc. 150 (2003) A330–A334.
[13] W. Choi, J.Y. Lee, H.S. Lim, Electrochem. Commun. 6 (2004) 816–820.
[14] I.A. Courtney, J.R. Dahn, J. Electrochem. Soc. 144 (1997) 2045–2052.
[15] J. Chouvin, J. Olivier-Fourcade, J.C. Jumas, B. Simon, P. Biensan, F.J. Fernández-Madrigal, J.L. Tirado, C. Pérez-Vicente, J. Electroanal. Chem. 494 (2000) 136–146.
[16] J. Li, H. Li, Z. Wang, L. Chen, X. Huang, J. Power Sources 107 (2002) 1–4.
[17] H. Li, X.J. Huang, L.Q. Chen, Electrochem. Solid State Lett. 1 (1998) 241–243.
[18] H. Li, L.H. Shi, W. Lu, H.J. Huang, L.Q. Chen, J. Electrochem. Soc. 148 (2001) A915–A922.
[19] M. Wachtler, J.O. Besenhard, M. Winter, J. Power Sources 94 (2001) 189–193.
[20] S. Leroy, F. Blanchard, R. Dedryvère, H. Martinez, B. Carré, D. Lemordant, D. Gonbeau, Surf. Interface Anal. 37 (2005) 773–781.
[21] R. Dedryvère, L. Gireaud, S. Grugeon, S. Laruelle, J.M. Tarascon, D. Gonbeau, J. Phys. Chem. B 109 (2005) 15868–15875.